Presented at the 29th European PV Solar Energy Conference and Exhibition, 22-26 September 2014, Amsterdam (NL)

INKJET-PRINTED DIFFUSION SOURCES

D.Stüwe[1,4], R. Keding, [1], A. Salim[1], M. Jahn[1], R. Efinger[1], F. Clement[1], B. Thaidigsmann[1], J. G. Korvink[2], C. Tueshaus[3], S. Barth[3], O. Doll[3] and D.Biro[1]

[1]Fraunhofer Institute for Solar Energy Systems (ISE), Heidenhofstrasse 2, 79110 Freiburg, Germany
[2]Merck KGaA, Frankfurter Str. 250, 64293 Darmstadt, Germany
[3]University of Freiburg - IMTEK, Georges-Köhler-Allee 102, 79110 Freiburg, Germany
[4]now with Notion Systems GmbH, Robert-Bosch-Str. 3-5, 68723 Schwetzingen, Germany

ABSTRACT: This paper presents an up-scalable solution for the formation of doped areas based on inkjet printing of boron and phosphorous doping inks. The influence of the thickness of the inkjet-printed doping source layers and the diffusion temperature on the sheet resistance is evaluated. In addition, the doping profiles are measured. For a diffusion temperature of 950 °C a sheet resistance of 50 Ω/sq is achieved with the boron ink. At the same temperature a sheet resistance of 18 Ω/sq is achieved with the boron ink. The process is then for the first time applied for the fabrication of back-contact back-junction solar cells with inkjet-printed p^+-emitter. The best solar cell features an efficiency of $\eta = 20.6$ %. To date, these are the best solar cells with an inkjet-printed doping source. Lifetime samples that are processed in parallel exhibit an emitter saturation current density below 90 fA/cm^2.
Keywords: inkjet, diffusion, BC-BJ

1 MOTIVATION

Inkjet-printed of phosphorus doping sources are reported in few publications. [1-6] The focus is on the one hand the selective emitter formation. Inkjet printing of boron doping sources is only reported by Kyungusn et. al..[7, 8] In this article the focus is on the use of inkjet-printing for the creation of doped phosphorus and boron regions aiming at the application for back-contact back-junction (BC-BJ) solar cells. BC-BJ solar cells feature multiple doped areas, namely the *n*-front surface field, the n^+-back surface field and the p^+-emitter. Usually the fabrication of such a solar cell requires many structuring steps and often more than one cost intensive high temperature step. Regarding the diffusion, the implementation of a co-diffusion process and of inkjet-printing doping sources allows for decreasing the number of process steps. [9-11]

2 INKJET-PRINTING OF DOPANT SOURCES

In this section, the development of the diffusion process from a boron ink (*B-ink*) and a phosphorus ink (*P-ink*) is described. The aim is the implementation inkjet-printed doping sources for the fabrication of BC-BJ solar cells. The first parameter that are varied is the thickness h of the inkjet-printed doping source layer that is adjusted with the printing resolution. The second parameter is the plateau temperature T_p of the diffusion process. The doped areas are characterized regarding the sheet resistance and the doping profile.

2.1 Sample preparation

The experiments for the evaluation of the doping process with the *B-ink* and the *P-ink* are performed on Cz-Si wafers with an edge length of 156 mm and a damage-etched surface, a wafer thickness of $h_W \approx 160$ µm and a base resistivity of $\rho \approx 2.2$ Ωcm. The experiment plan is depicted in Figure 1. To prevent doping of the wafer's rear side, it is covered by a thick SiO_2-layer. On the day, printing is performed, the wafers are dipped in an aqueous solution of 1% HF in order to remove native oxide and to guarantee a defined surface. For inkjet-printing a *PixDro LP50* equipped with a *Spectra SE 128-AA* printhead with 128 nozzles and a nominal droplet volume of $V_d = 30$ pl is used.

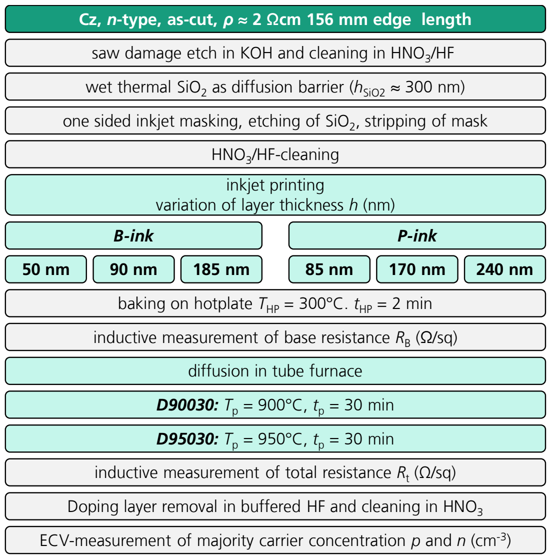

Figure 1 Process flow for the investigation of the influence of the thickness of the boron and phosphorus doping layers and the diffusion plateau temperature on the sheet resistance and the doping profile.

By a variation of the printing resolution the amount of ink is varied which results in three different thickness values. Each variation is printed on an area of approximately $A = 40 \times 40$ mm^2. Several variations are realized on the same wafer. After printing, the wafers are placed on a hotplate at a temperature of $T_{HP} = 300$ °C for $t_{HP} = 120$ s in order to burn off the organic components. Diffusion is performed in a tube furnace. The thickness of the dopant layers is measured on nine spots after diffusion by laser ellipsometry at a fixed wave length of 632 nm. Two plateau temperatures T_p are evaluated. Aiming for industrially relevant processing times, temperatures below 900 °C are not suitable due to the relatively slow diffusion of B into Si. The plateau temperatures chosen in this work are 900 °C and 950 °C. In both cases the plateau time t_s is 30 minutes. The recipes are referred to as *D90030* and *D95030* in this work.

The diffusion profiles are chosen in a way that they are suitable for the fabrication of a BC-BJ solar cell or a bi-facial *n*-type solar cell. [9-11] The sheet resistance is determined inductively after diffusion. Subsequently, the dopant glass layers are removed in a buffered solution of hydrofluoric acid (HF), and the carrier concentration profiles are determined by electrochemical capacity voltage (ECV) profiling.

2.2 Influence of the layer thickness

B-ink

By varying the doping source layer thickness, the transition between an exhaustible and an inexhaustible doping source can be regulated.

In Figure 2 the inductively measured R_{Sh}-values in dependence of the dopant layer thickness are depicted.

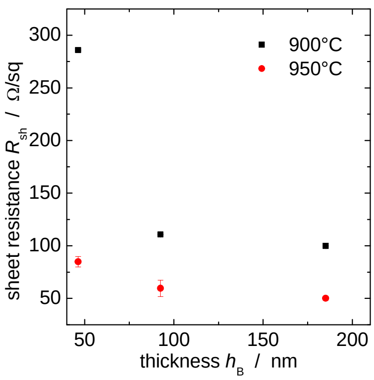

Figure 2 Sheet resistance in dependence of the thickness of the B doping layer for the recipes *D90030* and *D95030*.

For the diffusion *D90030* the thinnest layer results in a sheet resistance of $R_{Sh} = 286$ Ω/sq. The sheet resistance drops to $R_{Sh} = 111$ Ω/sq for $h_B \approx 90$ nm and $R_{Sh} = 100$ Ω/sq for $h_B \approx 185$ nm. A qualitatively similar behavior is observed for the diffusion *D95030*, however the span of R_{Sh}-values is narrower. There, the thinnest layer results in a sheet resistance of $R_{Sh} = 85$ Ω/sq, which drops to $R_{Sh} = 59$ Ω/sq and $R_{Sh} = 50$ Ω/sq for $h_B \approx 90$ nm and $h_B \approx 185$ nm.

In summary: for $h_B \approx 50$ nm, the doping source layer acts as an exhaustible diffusion source. For all diffusion recipes, an inexhaustible diffusion source is generated for a thickness between $h_B \approx 90$ nm and $h_B \approx 185$ nm.

P-ink

The R_{Sh}-values in dependence of the dopant layer thickness are depicted in Figure 3.

For *D90030* and *D95030* the sheet resistance values are constant and vary only slightly between $R_{sh} = 27$ Ω/sq - 33 Ω/sq and $R_{sh} = 13$ Ω/sq - 15 Ω/sq, respectively.

In all cases the inkjet-printed doping source layer acts as an inexhaustible doping source.

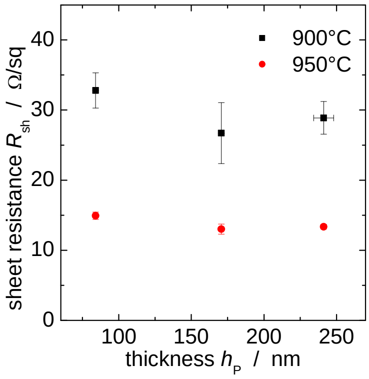

Figure 3 Sheet resistance in dependence of the thickness of the P doping layer for the recipes *D90030* and *D95030*.

2.3 Influence of the diffusion temperature

B-ink

Besides the sheet resistance measurements, doping profiles are measured by means of ECV in order better to show the influence of the diffusion temperature. For higher temperatures the solubility of boron atoms in Si increases, which leads to a higher surface concentration of boron (acceptor) atoms. In addition, the dopants diffuse deeper into the Si-wafer. Figure 4 shows the carrier concentrations for a layer thickness of $h_B \approx 185$ nm from the diffusion recipes *D90030* and *D95030*. The depicted R_{Sh}-values are calculated from the doping profiles. The surface concentration at 900 °C is $p = 6.9 \times 10^{19}$ cm^{-3}. At 950 °C the surface concentration is $p = 5.8 \times 10^{19}$ cm^{-3}. The depth of the doping profile increases with the temperature from approximately 0.3 µm to 0.5 µm. The sheet resistance decreases from $R_{Sh} = 110$ Ω/sq to $R_{Sh} = 49$ Ω/sq.

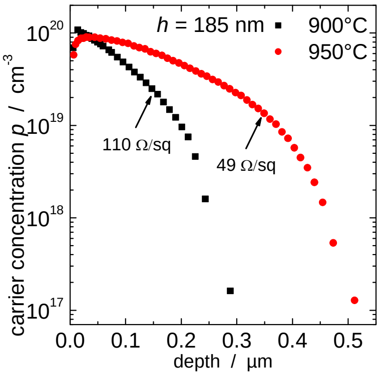

Figure 4 Doping profiles resulting from B doped layers with a thickness $h = 185$ nm for the diffusion recipes *D90030* and *D95030*. The graphs also include the sheet resistance values calculated from the doping profiles.

P-ink

The doping profiles achieved with the *P-ink* with a thickness of $h_P = 170$ nm are depicted in Figure 5. The surface concentration of P is for both diffusion recipes approximately $n = 3.8 \times 10^{20}$ cm^{-3}. The depth increases from approximately 0.7 µm to 1.2 µm.

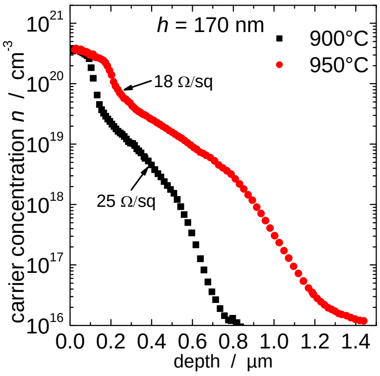

Figure 5 Doping profiles achieved from P doping layers with a thickness of $h = 170$ nm for the diffusion recipes *D90030* and *D95030*. The graphs also include the sheet resistance values calculated from the doping profiles.

3 BC-BJ SOALR CELLS WITH INKJET-PRINTED BORON p^+-EMITTER

3.1 Sample preparation

Solar cell fabrication, is conducted on samples that are produced following the scheme described by Keding et al..[10, 11] The process flow of the BC-BJ solar cells is depicted in Figure 6.

N-type Cz-wafers with an edge length of 156 mm and a base resistivity of 3.7 Ωcm are used as starting material. The BC-BJ precursors exhibit a textured front side and a full area doping source for the *n*-front surface field (FSF), as well as the patterned source for the *n*-back surface field, both deposited by plasma enhanced chemical vapor deposition (PECVD). Inkjet-printing is performed with a *PixDro LP50* inkjet printer equipped with a *Spectra SE-128AA* printhead with a nominal drop volume of 30 pl. On the rear, the *B-ink* is printed over the complete wafer surface. This is followed by a drying step on a hotplate for 120 s at a temperature of 300 °C in order to burn the organic solvents. Diffusion is performed in a tube furnace with the diffusion recipe *D95030*. This is followed by the removal of the doping source layer in a solution of buffered HF and a cleaning step in HNO_3. On the front surface a stack of a silicon rich oxy-nitride (SiriON) with a thickness of 6 nm and SiN_x:H with a thickness of 70 nm is deposited b PECVD. On the rear, a thin layer of Al_2O_3 with a thickness of 4 nm is deposited by atomic layer deposition, followed by the deposition of SiN_x:H with a thickness of 70 nm. The contact openings are etched in buffered HF and an inkjet printed etch resist is used for patterning. After etching, the ink is removed in an alternating stripping cascade of acetone and isopropyl alcohol (IPA), followed by a DI-water rinsing step. For the rear metallization, Al-Si (1%) with a thickness of 3000 nm is evaporated by e-gun. The metal-alloy layer is also structured by the inkjet mask and etch process. Etching of the Al-Si is performed in commercially available solution from Microchemicals. One wafer consists of 25 single solar cells with an area of 25 x 28 mm, that are cut out of the wafer using a laser. In order to form an electrical contact a tempering step is performed on a hotplate at $T_t = 400$ °C for $t_t = 30$s. Then the IV-curve is measured.

Lifetime samples are processed in parallel to the solar cells using the same Cz base material. However, there are some differences in the processing. First, these wafers exhibit a damage-etched surface, which is created by an etching step in KOH. The damage-etched surface is necessary, as it represents the rear face of the BC-BJ solar cell. Second, the *B-ink* is inkjet printed on both sides of the wafer in order to obtain symmetrical lifetime samples. After each printing step the wafer is dried on a hotplate at $T_{HP} = 300$ C for $t = 120$ s. The effective lifetimes τ_{eff} are measured using the quasi-steady-state photoconductance (QSSPC) method with a *Sinton WTC 120* from Sinton Instruments. Measurements are performed on nine spots across the wafer area. The dark saturation current density $j_{0,p+}$ is calculated with the slope method under high-level injection at an injection density of $\Delta n = 1 \times 10^{16}$ cm^{-3}.

$$j_{0,p+} = \frac{1}{2} q w n_i^2 \frac{d}{d\Delta n}\left(\frac{n_{i,eff}^2}{\tau_{corr}}\right) \qquad \textit{Equation 1}$$

with the elementary charge q, the wafer thickness w, the intrinsic carrier density n_i, the auger-corrected carrier lifetime τ_{corr}, the injection density Δn, and the injection dependent effective carrier density $n_{i,eff}$.

The maximum value of the open circuit voltage $V_{oc,limit}$ can be calculated by

$$V_{OC,limit} = \frac{k_B \times T}{q} \ln\left(\frac{j_{sc}}{j_{0,p+}} + 1\right) \qquad \textit{Equation 2}$$

with the Boltzmann constant k_B and the short circuit current density jsc.

The measurement is performed directly after deposition of the passivation layers and after several tempering steps. Tempering is performed on a hotplate at a temperature of $T_t = 400$ °C. the tempering time is varied and the following values are chosen: $t_t = 30$ s, 60 s, 120 s, 240 s and 480 s.

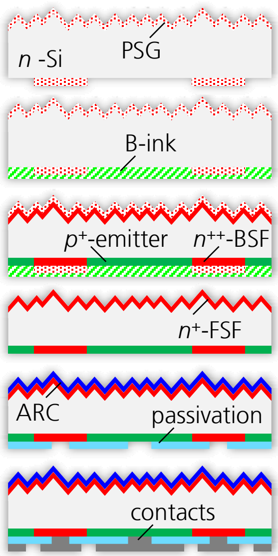

Figure 6 Schematic process flow for the fabrication of BC-BJ solar cells using the *B-ink*.

3.2 Solar cell results

For the IV-curve measurement the solar cell´s front side is covered with a mask having an aperture area of 19.685 mm^2, which covers the busbars. This allows for the measurement of the active cell area only. The first solar cell measurement is performed directly after deposition of the Al-Si (1%) metal alloy and the laser cutting. With some cells of the same experiment an evaluation of the tempering time is performed, which show that already after a tempering time of $t_t = 60$ s at $T_t = 400$ °C, the efficiency values drop, caused mainly by a decrease of the *FF*. Thus, for the other cells a tempering time of $t_t = 30$ s is used. The solar cell results for a sample with inkjet-printed *p*+-emitter are listed in Table 1. In the non-tempered process stage, an efficiency of only $\eta = 18.6$ % is obtained. This is very likely due to insufficient contact formation. After the tempering step the open circuit voltage and the short circuit current density rise to $V_{oc} = 654$ mV and $j_{sc} = 41.5$ mA/cm^2, respectively and result in an efficiency of $\eta = 20.6$ %.

Table 1 Solar cell parameters of the first BC-BJ solar cells with inkjet-printed *p*+-emitter.

tempered	V_{oc} (mV)	j_{sc} (mA/cm^2)	*FF* (%)	η (%)
no	610	40.6	75.2	18.6
yes	654	41.5	76	20.6

To date this is the first BC-BJ solar cell with an inkjet-printed p^+-emitter. In addition, it is the best solar cell result, ever reported featuring an inkjet-printed diffusion source.

Regarding the lifetime samples, the average $j_{0,p+}$-value rises slightly from $j_{0,p+} = 101$ fA/cm^2 at the non-tempered stage to $j_{0,p+} = 105$ fA/cm^2 for $t_t = 60$s. It decreases to $j_{0,p+} = 86$ fA/cm^2 for $t_t = 480$s. The results show, that very high $V_{oc,\ limit}$-values of approximately 690 mV can be achieved. This makes the inkjet printing process very promising to be further evaluated for the BC-BJ solar cell.

4 SUMMARY

In this article a diffusion processes for the realization of boron and phosphorus doped areas using inkjet-printed doping sources is developed. The thickness of the doping source layers can be adjusted by the drop density. The influence of the doping layer thickness and the diffusion temperature on the sheet resistance and the doping profiles are evaluated. For a diffusion temperature of 950 C a sheet resistance of 50 Ω/sq is achieved with the boron ink. At the same temperature, a sheet resistance of 18 Ω/sq is achieved with the boron ink.

For the first time, BC-BJ solar cells with inkjet-printed p^+-emitter are presented. The best solar cell features an open circuit voltage $V_{oc} = 654$ mV, a short circuit current density $j_{sc} = 41.5$ mA, a fill factor $FF = 76$ % and an efficiency $\eta = 20.6$ %. These are to date the best solar cells with an inkjet-printed doping source. The implementation of inkjet-printed doping sources allows for a drastic reduction of processing steps of BC-BJ solar cells. These results pave the way for future work, where BC-BJ solar cells are fabricated with *p*+-emitter and the *n*+-BSF, simultaneously applied by inkjet-printing.

6 ACKNOWLEDGEMENTS

Thanks goes to the whole PVTEC-team for processing and the whole Merck-team for providing the inks and support.

6 REFERENCES

1. Xu, H.X., et al. *Printable dopant materials for solar cell applications*. in *Proceedings of the 26th European Photovoltaic Solar Energy Conference and Exhibition*. 2011. Hamburg, Germany.
2. Tormey, E., et al. *Inkjet fabrication of shallow emitters in silicon solar cells* in *Proceedings of the 25th European Photovoltaic Solar Energy Conference and Exhibition*. 2010. Valencia, Spain.
3. Mrcarica, M., et al. *Dopant deposition techniques and their impact on emitter formation in high efficiency and high throughoutput in-line doping/diffusion system*. in *Proceedings of the 26th European Photovoltaic Solar Energy Conference and Exhibition*. 2011. Hamburg, Germany.
4. Khaselev, O., et al. *Novel inkjet inks for complete off contact fabrication of silicon solar cell*. in *Proceedings of the 23rd European Photovoltaic Solar Energy Conference*. 2008. Valencia, Spain.
5. Chen, T., et al. *NOVEL SELECTIVE-EMITTER SOLAR CELLS FABRICATION USING INERT PIEZOELECTRIC INKJET TECHNOLOGY*. in *Proceedings of the 27th European Photovoltaic Solar Energy Conference and Exhibition*. 2012. Frankfurt, Germany.
6. Antoniadis, H. *Silicon Ink high efficiency solar cells*. in *Photovoltaic Specialists Conference (PVSC), 2009 34th IEEE*. 2009.
7. Kyungsun, R., et al., *High-Efficiency n-Type Si Solar Cells With Novel Inkjet-Printed Boron Emitters.* Electron Device Letters, IEEE, 2012. 33(6): p. 854-856.
8. Kyungsun, R., et al. *High efficiency n-type silicon solar cell with a novel inkjet-printed boron emitter*. in *Photovoltaic Specialists Conference (PVSC), 2011 37th IEEE*. 2011.
9. Rothhardt, P., et al., *Co-diffusion from APCVD BSG and* $POCl_3$ *for Industrial n-type Solar Cells.* Energy Procedia, 2013. 38(0): p. 305-11.
10. Keding, R., et al. *Co-diffused back-contact back-junction silicon solar cells*. in *Proceedings of the 28th European Photovoltaic Solar Energy Conference and Exhibition*. 2013. Paris, France.
11. Keding, R., et al., *Co-Diffused Back-Contact Back-Junction Silicon Solar Cells without Gap Regions.* Photovoltaics, IEEE Journal of, 2013. PP(99): p. 1-7.